Applied Mathematics and Computation 237 (2014) 227–237

Contents lists available at ScienceDirect

Applied Mathematics and Computation

journal homepage: www.elsevier.com/locate/amc

A nonlinear model of the dynamics of radial dislocations in microtubules

S. Zdravković [a,*], M.V. Satarić [b], A. Maluckov [a], A. Balaž [c]

[a] Institut za nuklearne nauke Vinča, Univerzitet u Beogradu, Poštanski fah 522, 11001 Beograd, Serbia
[b] Fakultet tehničkih nauka, Univerzitet u Novom Sadu, 21000 Novi Sad, Serbia
[c] Institut za fiziku, Univerzitet u Beogradu, Pregrevica 118, 11080 Beograd, Serbia

ARTICLE INFO

Keywords:
Microtubule
Radial degree of freedom
Partial differential equation
Kink soliton

ABSTRACT

We have established a new dynamical model of microtubules based on their intrinsic dipolar character. The model assumes a single angular degree of freedom per dimer describing the conformational displacements of constituent dimers in radial direction. A corresponding nonlinear dynamical equation of motion is solved both analytically, using the simplest equation method, and numerically. It is shown by both approaches that kink solitons could be elicited and sustained to propagate along the microtubule. We suggest that this model could explain some dynamical functional properties of microtubules, including the triggering of the onset of their depolymerization.

1. Introduction

Microtubules (MTs) form an important part of the cellular skeleton and represent a network for intracellular transport of motor proteins. They also play a crucial role during cell division, forming a dynamic structure that spatially separates duplicated chromosomes.

Microtubules represent hollow cylinders formed by protofilaments (PFs) aligned in directions that are parallel to their axes [1–5]. There are in vivo usually 13 longitudinally ordered PFs covering the cylindrical walls of MTs. The lengths of MTs span dimensions from the order of micrometers to the order of millimetre. The approximate values of the outer and the inner radii of MT cylinder are 25 nm and 15 nm, respectively [6–8].

PF represents a series of proteins known as tubulin heterodimers. Each dimer is effectively an electric dipole whose length is $l = 8$ nm, as shown in Fig. 1. Its electric dipole moment and charge displacement are: $p = 337\text{Debye} = 1.13 \times 10^{-27}$ Cm and $d \approx 4$ nm, respectively [6,9–11].

Microtubules are very dynamic polymers whose polymerization and disassembly are determined by whether their dimers are in a straight position within PFs or in radially displaced positions pointing out of cylindrical surface. These circumstances are the basis for our attempt to describe MT dynamics relying on the nonlinear model expressed by this single degree of radial displacement of tubulin dimer within PF.

The paper is organized as follows. In Section 2 we establish the nonlinear model of collective conformations of the dimers within PF. Section 3 deals with the analytical solution of equation of motion in terms of the simplest equation method. The numerical solutions of higher-order expansion of cosine function are presented in Section 4. The conclusions including the possible biological implications are presented in Section 5.

* Corresponding author.
E-mail address: szdjidji@vinca.rs (S. Zdravković).

http://dx.doi.org/10.1016/j.amc.2014.03.113
0096-3003/

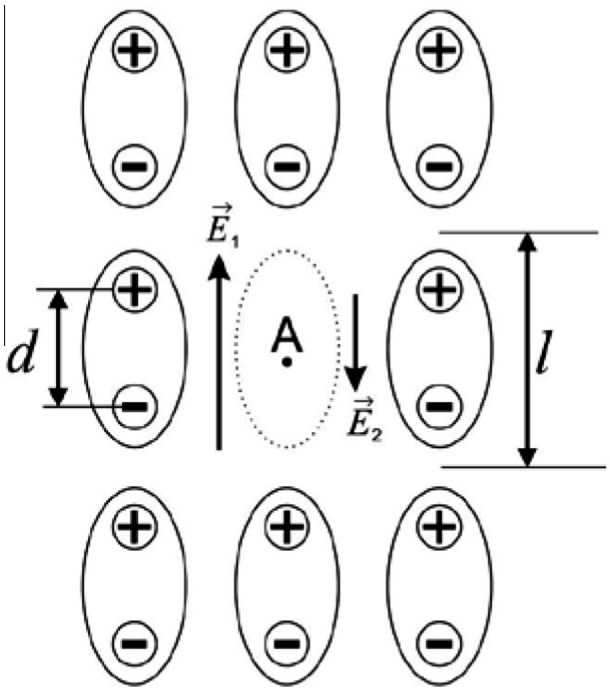

Fig. 1. A segment of three protofilaments (PF1, PF2 and PF3, from left to right) with the fields $\vec{E}_1$ and $\vec{E}_2$ in the point A, arising from the same protofilament PF2 and from the neighbouring PFs, respectively. The dipole moment $\vec{p}$ of the tubulin dimer has the displacement of the opposite charges depicted with d.

2. Dynamical model of microtubules

A simplified picture, relevant for the model established in this paper, is shown in Fig. 1. Let us consider the dimer in the middle, belonging to PF2. It feels electric fields of the neighbouring dimers. The field $\vec{E}_1$ comes from the dimers belonging to the same PF2, while $\vec{E}_2$ is the longitudinal component of the field which originates from the dimers belonging to the neighbouring PFs, i.e. PF1 and PF3. Details about the calculations of the above fields are published in Ref. [12]. It might be noticed that PF1 and PF3, in Fig. 1, should be respectively displaced up and down in order to match the real MT structure, i.e. its intrinsic helicity. These displacements lead to a component of $\vec{E}_{2p}$ in perpendicular direction to $\vec{E}_1$. However, the component $\vec{E}_{2p}$ is not taken into account in the present model as being irrelevant for the considered degree of freedom.

The tubulin dimers within PFs can perform conformational changes that may propagate along either individual PFs or small groups of PFs. The bending of PFs during disassembly of MT is the consequence of such cooperative conformations [13]. It was shown that the relative displacement of two neighbouring dimers can reach 32° prior disrupting PF. In addition, the angular displacements of the monomers within a single dimer can be up to 13° [14]. These facts motivated us to restrict our modeling to the angular conformations of dimers φ in radial directions from the line of the dipolar electric field $\vec{E} = \vec{E}_1 + \vec{E}_2$. Therefore, we assume that the whole dimer rotates and the corresponding angular displacement is φ. What the point is, around which this rotation occurs, is not known in this moment. It may be a dimers tip, its centre or any point in between. This is only important for the estimation of its moment of inertia, which is beyond the topic of this paper.

A dipolar potential energy of a single dimer is simply expressed as a scalar product

$$U(\varphi) = -\vec{p}\cdot\vec{E} = -qdE\cos\varphi, \tag{1}$$

where q represents the excess charge of the monomer within the dipole. It is assumed that the inequalities $p > 0$ and $E > 0$ hold.

In the nearest neighbour approximation, the expression for the Hamiltonian of one PF in a discrete version is

$$H = \sum_n \left[\frac{I}{2}\dot{\varphi}_n^2 + \frac{k}{2}(\varphi_{n+1} - \varphi_n)^2 - pE\cos\varphi_n\right], \tag{2}$$

which, after a series expansion of the cosine function, becomes

$$H = \sum_n \left[\frac{I}{2}\dot{\varphi}_n^2 + \frac{k}{2}(\varphi_{n+1} - \varphi_n)^2 - pE + pE\left(\frac{\varphi_n^2}{2} - \frac{\varphi_n^4}{24}\right)\right]. \tag{3}$$

Here the dot means a first derivative with respect to time, I is a moment of inertia of the single dimer and k stands for inter-dimer bonding interaction within the same PF, which is provided by the link between the corresponding protruding loops [15]. The integer n determines the position of the dimer in the PF. It is obvious that the first term in Eqs. (2) and (3) represents the dimer's kinetic energy, while the second one is a potential energy of the chemical interaction between the dimers belonging to the same PF. The chemical interaction between the neighbouring dimers belonging to different PFs is much smaller and the corresponding energy is here safely neglected [16,17]. This does not mean that the influence of the neighbouring PFs is completely ignored since the field $\vec{E}_2$ just comes from these PFs, as explained above. This is very important fact since the magnitude of the electric moment $|\vec{p}|$ and the MT length l bring about the pretty big value for $\vec{E}_1$. Hence, the field $\vec{E}_2$, pointing in the opposite direction from $\vec{E}_1$, properly reduces the value of the total intrinsic field $\vec{E}$.

Using common generalized coordinate $q_n = \varphi_n$ and angular momentum $p_n = I\dot{\varphi}_n$, assuming the validity of a continuum approximation $\varphi_n(t) \to \varphi(x,t)$ and eventually taking a series expansion

$$\varphi_{n\pm1} \to \varphi \pm \frac{\partial\varphi}{\partial x} l + \frac{1}{2}\frac{\partial^2\varphi}{\partial x^2} l^2 \tag{4}$$

we can straightforwardly obtain an appropriate dynamical equation of motion. If a viscosity momentum $M_v = -\Gamma\dot{\varphi}$, where Γ stands for the viscosity coefficient, is adequately incorporated into the equation of motion, we obtain, according to Eq. (3), a following partial differential equation (PDE)

$$I\frac{\partial^2\varphi}{\partial t^2} - kl^2\frac{\partial^2\varphi}{\partial x^2} + pE\varphi - \frac{pE}{6}\varphi^3 + \Gamma\frac{\partial\varphi}{\partial t} = 0. \tag{5}$$

It is well known that an ordinary differential equation (ODE) can be obtained from Eq. (5) just introducing a unified coordinate ξ defined as usual

$$\varphi(x,t) = \varphi(\xi) \equiv \varphi(\kappa\, x - \omega\, t), \tag{6}$$

where κ and ω are constants, meaning the wave number and the frequency, respectively. Therefore, by combining Eq. (6) and a suitable transformation

$$\varphi = \psi\sqrt{6} \tag{7}$$

we can easily transform Eq. (5) into the following ODE

$$\alpha\frac{d^2\psi}{d\xi^2} - \rho\frac{d\psi}{d\xi} + \psi - \psi^3 = 0, \tag{8}$$

where the two dimensionless parameters α and ρ underlay physics of the pertaining model as follows

$$\alpha = \frac{I\omega^2 - kl^2\kappa^2}{pE}, \quad \rho = \frac{\omega\Gamma}{pE}. \tag{9}$$

The parameter α represents the measure of competition between rotational kinetic energy of the tubulin dimer and its potential energy of pertaining chemical bonds, additionally balanced by the strength of intrinsic electric field $\vec{E}$. The softness of chemical bonds and the strong increase of dimer's kinetic energy [18], caused by a release of 0.25 eV of energy produced by GTP hydrolysis, yields that the parameter α must be positive. This means that kinetic energy should prevail, but the presence of additional dipolar potential is sufficient to prevent the degradation of PF when such excitation is away from MT ends. This fact indicates that dipolar potential energy does play the decisive role in stabilizing of PFs and MT itself, thus sustaining the polymerization. In what follows we assume that ρ is known and determine the crucial parameter α.

Before we proceed we want to compare Eq. (1) with the earlier models dealing with nonlinear dynamics of MTs. In Ref. [3] the angular coordinate φ was also used but the corresponding double-well potential is just postulated in the celebrated Landau-Ginsburg version

$$f_0(\varphi) = -\frac{A}{2}\varphi^2 + \frac{B}{4}\varphi^4, \quad A > 0,\ B > 0. \tag{10}$$

In Ref. [5] a longitudinal degree of freedom u_n was established instead of φ_n and the potential energy of the form given by Eq. (10) was also assumed. We argue that the present approach is more realistic since the intrinsic dipolar electrostatic energy within MT is properly taken into account.

We stress here that the last three terms in Eq. (3) are coming from the series expansion of the cosine function which is not disputable. Of course, the number of the terms in this series expansion is pretty crucial. It will be elaborated in very details later on, in Section 4.

The explained model is obviously the radial one. It might be interesting to mention that longitudinal models have been introduced as well [5,12,19]. All of them assume only one degree of freedom per dimer. An extension, which would take more than one degree of freedom, is very interesting but also a tough job. This requires further research and is not the topic of this paper.

3. Analytical solutions of Eq. (8)

Eq. (8) can be solved analytically using a few mathematical procedures. A couple of examples for those methods can be a standard procedure [5,20], extended tanh-function method [21–25], a procedure based on Jacobian elliptic function [26–28] and a method of factorisation [29–32]. In this paper we are using the simplest equation method (SEM), which is more general than any of the aforementioned procedures.

According to SEM we look for the possible solution of Eq. (8) in the form of a trial function ψ

$$\psi = A_0 + \sum_{k=1}^{N}\left(A_k\Phi^k + B_k\left(\frac{\Phi'}{\Phi}\right)^k\right), \tag{11}$$

where A_0, A_k and B_k are coefficients that should be determined and Φ' represents the first derivative. The function Φ is a known solution of a so-called the simplest equation [33,34]. The simplest equation can be any nonlinear ordinary differential equation of lower order than Eq. (8) with the known general solution. In this paper for the simplest equation we chose the Riccati equation [33]

$$\Phi' + \Phi^2 - 2a\Phi - b = 0, \quad a, b = \text{const}. \tag{12}$$

To determine the positive integer N in Eq. (11) we should plug $\psi = c/\xi^p$ in Eq. (8) and concentrate our attention on the leading terms [35]. These are the terms that lead to the least positive p and the balance of all the leading terms provides us with the value of N. One can easily show that $N = 1$ for Eq. (8).

To obtain the final expression for the function ψ we need to determine the values of the parameters b, A_0, A_1 and B_1. Also, we are looking for α, as was mentioned above. From Eqs. (11) and (12) we can obtain the expressions for ψ', ψ'' and ψ^3. All this brings about the following expression

$$K_0 + K_1\Phi + K_1'\Phi^{-1} + K_2\Phi^2 + K_2'\Phi^{-2} + K_3\Phi^3 + K_3'\Phi^{-3} = 0, \tag{16}$$

which is satisfied if all the coefficients are simultaneously equal to zero. This brings about a system of seven equations. Two of them are

$$K_3 \equiv 2\alpha A_1 - A_1^3 - 2\alpha B_1 + 3A_1^2B_1 - 3A_1B_1^2 + B_1^3 = 0, \tag{17}$$

and

$$K_3' \equiv 2\alpha b^3 B_1 - b^3 B_1^3 = 0. \tag{18}$$

Eq. (17) can be written as

$$(B_1 - A_1)[(B_1 - A_1)^2 - 2\alpha] = 0, \tag{19}$$

which determines the following two cases.

$$\text{Case 1.} \quad B_1 = A_1 \tag{20}$$

Eqs. (18) and (20) reduce the system mentioned above to the simpler one

$$\left.\begin{aligned} &-3aA_1^2 - 3A_1A_0 + \rho = 0 \\ &1 - 10a^2A_1^2 - 12aA_1A_0 - 3A_0^2 - A_1^2b + 2a\rho = 0 \\ &2aA_1 - 8a^3A_1^2 + A_0 - 12a^2A_1^2A_0 - 6aA_1A_0^2 - A_0^3 - aA_1^3b - A_1b\rho = 0 \end{aligned}\right\}, \tag{21}$$

where $b \neq 0$ is assumed. Using Mathematica or a similar software we easily obtain the following two solutions

$$A_0^{(1)} = \frac{1}{6}(3 - 4a\rho), \quad A_1^{(1)} = \frac{2\rho}{3} \tag{22}$$

and

$$A_0^{(2)} = -\frac{1}{6}(3 - 4a\rho), \quad A_1^{(2)} = -\frac{2\rho}{3}. \tag{23}$$

For the both solutions the expressions for the remaining two parameters are

$$b = \frac{9 - 16a^2\rho^2}{16\rho^2}, \quad \alpha = \frac{2\rho^2}{9} \tag{24}$$

$$\text{Case 2.} \quad \alpha = \frac{(A_1 - B_1)^2}{2} \tag{25}$$

Eqs. (18) and (25) yield to

$$A_1 = 2B_1, \tag{26}$$

which reduces the initial system to the system of five equations. This system can be solved only if

$$a = 0, \tag{27}$$

which brings about the system

$$\left.\begin{aligned} &-3A_0B_1 + \rho = 0\\ &1 - 3A_0^2 - 4bB_1^2 = 0\\ &A_0 - A_0^3 - 6A_0bB_1^2 - 2bB_1\rho = 0 \end{aligned}\right\}. \tag{28}$$

Its solutions are

$$A_0^{(1)} = \frac{1}{2}, \quad B_1^{(1)} = \frac{2\rho}{3} \tag{29}$$

and

$$A_0^{(2)} = -\frac{1}{2}, \quad B_1^{(2)} = -\frac{2\rho}{3}. \tag{30}$$

For the both solutions the expressions for the remaining two parameters are

$$b = \frac{9}{64\rho^2}, \quad \alpha = \frac{2\rho^2}{9}. \tag{31}$$

Therefore, the values of all necessary coefficients have been found. To obtain the expression for the function ψ we should know the function Φ. The well-known general solution of Eq. (12) is [33]

$$\Phi = a + \sqrt{a^2 + b}\tanh\left[\sqrt{a^2 + b}(\xi - \xi_0)\right]. \tag{32}$$

To obtain the expression (32) we can plug a trial function

$$\Phi = C + C_1\tanh[C_2(\xi - \xi_0)], \tag{33}$$

where C, C_1 and C_2 are constants, into Eq. (12), which brings about $C = a$, $C_2 = C_1$ and $C_1^2 = a^2 + b$. Some more information about the general solution of the Riccati equation can be found in Refs. [36,37]. In what follows $\xi_0 = 0$ will be assumed.

Finally, we can write the expressions for the function ψ. Let ψ_1 and ψ_2 be the values of ψ for the cases 1 and 2, respectively. To obtain ψ_1 we should use Eqs. (20), (22)–(24) and (32) while Eqs. (26), (27), (29), (30), (31), and (32) yield ψ_2. These functions are

$$\psi_1(x,t) = \pm\frac{1}{2}\left[1 + \tanh y + \frac{1}{\cosh^2 y(d + \tanh y)}\right] \tag{34}$$

and

$$\psi_2(x,t) = \pm\frac{1}{2}\left[1 + \tanh\left(\frac{y}{2}\right) + \frac{1}{\sinh y}\right], \tag{35}$$

where

$$y = \frac{3}{4\rho}(\kappa x - \omega t). \tag{36}$$

To obtain Eq. (34) the parameter d has been introduced through

$$a = \frac{3}{4\rho}d. \tag{37}$$

Obviously, ψ_2 does not have physical meaning as its last term diverges for $\xi = 0$. As for ψ_1 its denominator is different from zero for $d > 1$ and, of course, this solution may have physical meaning. This function is shown in Fig. 2 for three values of the parameter d, suggesting that a kink soliton moves along MT. The graph was plotted for the positive sign in Eq. (34). If we had chosen minus in Eq. (34) we would have obtained antikink soliton instead, which is physically equivalent. If $d = 1$, i.e. $a = \frac{3}{4\rho}$, then $\psi_1 = 1$ for any ξ.

To derive Eqs. (34) and (35) it was assumed that $b \neq 0$. For $b = 0$ direct integration of Riccati equation brings about

$$\Phi_0 = \frac{2a}{1 + e^{-2a\xi}}. \tag{38}$$

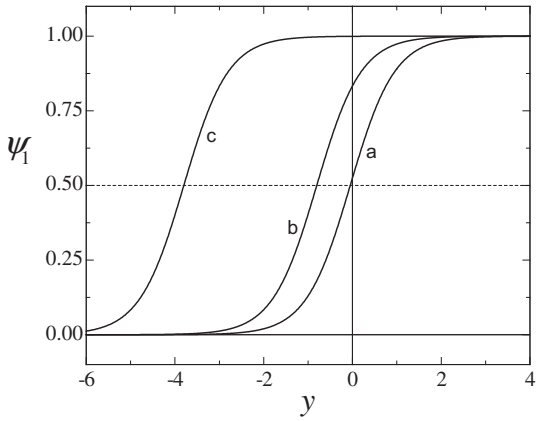

Fig. 2. Function ψ_1 for $\rho = 1$ and (a) $d = 20$, (b) $d = 1.5$ and (c) $d = 1.001$.

Of course, this is nothing but Φ given by Eq. (32) for $b = 0$. Following the same procedure as above we straightforwardly obtain trivial solutions for Eq. (8), that are $\psi = 0$ and $\psi = \pm 1$.

It is interesting to study the case $B_1 = 0$ in Eq. (11). This simplified version of SEM is nothing but extended tanh-function method [21–25]. Following the same procedure as above we obtain Eqs. (20)–(24) again. This brings about the final result

$$\psi(x,t) = \pm\frac{1}{2}[1 + \tanh y]. \tag{39}$$

If we plotted the functions ψ_1 and ψ, given by Eqs. (34) and (39), we would notice that these are practically equal but shifted functions. We can check if there is a certain shift δ for which

$$1 + \tanh(y+\delta) = 1 + \tanh y + \frac{1}{\cosh^2 y\,(d + \tanh y)} \tag{40}$$

holds. Using a formula

$$\tanh(y+\delta) = \frac{\tanh y + \tanh\delta}{1 + \tanh y \tanh\delta} \tag{41}$$

we straightforwardly obtain

$$\tanh\delta = \frac{1}{d}. \tag{42}$$

This is very interesting result indicating that the trial function (11), for our Eq. (8), could have been simpler without the third term. Its physical explanation is simple as both ψ_1 and ψ describe same physics. Namely, both functions represent kink solitons moving along PF with the same velocity and the shift is irrelevant.

A case $A_1 = 0$ corresponds to modified SEM [35,36]. This is less important as the mentioned system of seven equations can be solved only if $\rho = 0$, which is physically unacceptable.

Finally, according to Eqs. (7), (36), and (39) and for the positive sign in Eq. (39), we obtain

$$\varphi(x,t) = \frac{\sqrt{6}}{2}\left[1 + \tanh\left(\frac{3}{4\rho}(\kappa x - \omega t)\right)\right]. \tag{43}$$

It is obvious that the solitonic width of the above kink is proportional to viscosity of physiological surrounding and inversely proportional to pE, which can be seen from the second of Eq. (9).

The function $\psi(\xi)$ is shown in Fig. 3, together with numerical solutions of Eq. (8), which will be explained later.

On the basis of the first of Eq. (9) we can see how the parameter α depends on the solitonic and the linear sound velocities, denoted by v and c, respectively. Namely,

$$\alpha = \frac{I\kappa^2}{pE}(v^2 - c^2), \tag{44}$$

where

$$v = \frac{\omega}{\kappa}, \quad c^2 = \frac{kl^2}{I}. \tag{45}$$

As $\alpha > 0$ we see that the above soliton belongs to the class of supersonic solitons, well-known from literature [38]. Also, the expressions for α in Eqs. (9) and (24) yield the following useful relationship between v and c

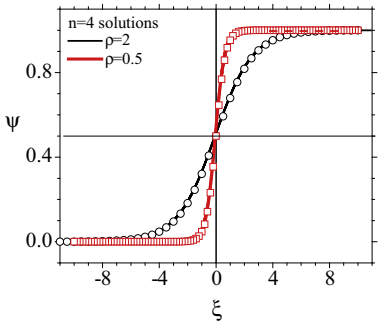

Fig. 3. The analytical (solid lines) and numerical (dots) solutions of Eq. (8) for $\rho = 0.5$ and $\rho = 2$. The values of the parameters α are given by Eq. (24).

$$v = \frac{c}{\sqrt{1 - \frac{2\Gamma^2}{9pEI}}} > c. \tag{46}$$

This demonstrates that we deal with the supersonic soliton and imposes the necessary inequality

$$9pEI > 2\Gamma^2. \tag{47}$$

4. Improved version of the model

Someone might complain that the series expansion of the cosine function may not be correct as the angle φ has big values, up to $\sqrt{6}$ rad. In fact, to derive Eq. (8) we kept all terms to order $n = 4$ in φ, which can be seen from Eq. (3). Higher-order expansions are obtained for larger values of n, and represent better approximations to the initial Hamiltonian. For $n = 6$ and $n = 8$ we get the equations of motion with the nonlinearities of the orders 5 and 7. The latter one is

$$\alpha\psi'' - \rho\psi' + \psi - \psi^3 + 0.3\psi^5 - \frac{0.3}{7}\psi^7 = 0, \tag{48}$$

instead of Eq. (8). The SEM method cannot be applied any more so that numerical solutions of equations for $n = 6$ and $n = 8$ are required. In what follows, the results of numerical calculations are presented. The ODE (48) (as well as Eq. (8)) is numerically solved by adopting standard shooting method with the Runge–Kutta integrator [39]. We found that good numerical convergence is guarantied for the value of the numerical step $h = 10^{-6}$, thus in the following numerical results are generated by it. We focused on solutions satisfying the following asymptotic conditions:

$$\psi(-\infty) = 0, \quad \psi(+\infty) = 1 \tag{49}$$

coming from Eq. (8) and the analytical solution. The numerical calculations had to start from the unstable attractor ($\psi_a = 1$) and to be carried out backwards via a negative step size, until the stable attractor ($\psi_a = 0$) is reached.

Fig. 3 represents a comparison of analytical and numerical solutions of the equation of motion for $n = 4$ microtubule model for two values of the parameter ρ. Perfect agreements of the analytic and the numeric solutions are obvious.

If we keep all the terms in the expansion of cosine up to order $n = 6$ in the Hamiltonian, the corresponding equation of motion is Eq. (48) without the last term. However, it does not admit horizontal asymptotes $\psi(\xi) \to \psi_a$ when $\xi \to \pm\infty$ as this equation has only one real solution $\psi_a = 0$ when the derivatives are zero. Therefore, $n = 6$ model cannot represent signal propagation along PF, which is assumed to interpolate between two distinct states (horizontal asymptotes).

Higher-order model corresponding to $n = 8$ leads to Eq. (48) which admits horizontal asymptotes. One can easily show that, apart from $\psi_a = 0$, the solution of Eq. (48) may have two more horizontal asymptotes and these are

$$\psi_a = \pm q, \quad q \approx 1.26 \tag{50}$$

This is shown in Fig. 4 where the solutions of Eqs. (8) and (48) are compared for $\rho = 2$ and α given by Eq. (24). We used the same numerical method as for Fig. 3. It is obvious that we were focused to the solution interpolating between 0 and q. One can see that the additional terms in Eq. (48) bring about a certain shift from 1 to q. The graph also shows asymptotic solutions of the linearized versions of Eqs. (8) or (48). This will be derived in a more elaborate version of this work. It suffices now to notice that these asymptotes nicely describe the asymptotical behaviour of the numerical solutions.

5. Conclusions and biological implications

In this article a new dipolar model describing the collective nonlinear dynamics of tubulin dimers within the MTs is introduced and elaborated. A very important and interesting result arises from the requirement for positive parameter α in Eq.

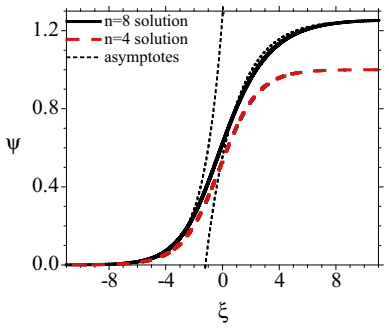

Fig. 4. Comparison of numerical solutions of the equations of motion for $n = 4$ and $n = 8$ microtubule model for $\rho = 2$. The value of the parameter α is given by Eq. (24).

(24). This implies that the inertial term (the first term in Eq. (5)) is larger than the second, elastic one. This is uncommon in solid state physics, but seems possible in typical biological soft matter structures. To understand this circumstance we should keep in mind that MTs are polymerized without strong covalent bonds. Instead, the links between dimers within PF are mostly on the basis of very soft hydrogen bonds [15,16]. This means that the value of the stiffness parameter k in Eq. (2) is adequately small.

It is also interesting to consider a case of balanced kinetic and elastic energy. Under these circumstances we set $\alpha = 0$. Then Eqs. (5), (7) and (9) bring about

$$\dot{\psi} = \frac{pE}{\Gamma}\psi(\psi - 1)(\psi + 1), \tag{51}$$

where the dot represents a first derivative with respect to time. If we apply a simple and standard stability analysis [40] we see that the point $\psi = 0$ is stable while the points $\psi = \pm 1$ are unstable. This certainly means that the state $\varphi(-\infty) = 0$ is stable (straight position of the dimers) while the strong angular conformation $\varphi(+\infty) = \sqrt{6}$ is unstable leading to depolymerisation of MT.

It might be interesting to point out that $\alpha = 0$ is not a rude approximation. To understand this we should compare the terms in Eq. (5) using Eqs. (9), (31), and (43). Hence, the first two terms and the linear one are respectively

$$I\frac{\partial^2\varphi}{\partial t^2} - kl^2\frac{\partial^2\varphi}{\partial x^2} = pE\sqrt{6}f_1(y), \tag{52}$$

and

$$pE\varphi(x,t) = pE\sqrt{6}f_2(y), \tag{53}$$

where y is given by Eq. (36). The function $f_2(y)$ is nothing but the function ψ shown in Fig. 3. According to Eqs. (5), (9), (31), and (43) we can see that

$$f_1(y) = -\frac{1}{8}\frac{\sinh y}{\cosh^3 y}. \tag{54}$$

This function is shown in Fig. 5. In the same way we can easily show that the first two terms are at least three times smaller than the viscosity one. All this certainly indicates that $\alpha = 0$ is not the rude approximation.

A direct integration of Eq. (51) yield the pertaining function

$$\psi_0^2 = \frac{e^\gamma}{1 + e^\gamma} = \frac{1}{2}\left[1 + \tanh\left(\frac{1}{\rho}(\kappa x - \omega t)\right)\right], \tag{55}$$

where the index zero indicates $\alpha = 0$ case. Notice a square of ψ_0 in Eq. (55). Fig. 6 shows both the function ψ corresponding to α given by Eq. (24) and the function ψ_0. It is obvious that both functions have equal physical meaning indicating again that $\alpha = 0$ is the appropriate approximation.

A question arises if Eq. (8) can be solved for the negative value of the parameter α. Apparently this cannot be done by SEM since this procedure brings about Eq. (24), i.e. positive α. But, on the basis of numerical approach it works and the solutions for both positive and negative α are presented in Fig. 7. It appears that the asymptotic behaviours are the same for all the three cases ($\alpha < 0$; $\alpha = 0$; $\alpha > 0$). All three functions are almost equal for small $|\xi|$ and the solution for $\alpha < 0$ exhibits damped oscillations before the asymptotic values are reached.

It is apparent from Eq. (43) that the conformational angle φ takes values from zero to $\sqrt{6}$ radians. Initially, in stable MT, all dimers are in the straight configuration along pertaining PFs. When energy of hydrolysis of GTP molecules is imparted to dimers the kink excitations should be created [18]. This means that the dimers rotate for the angle φ from the main axes in

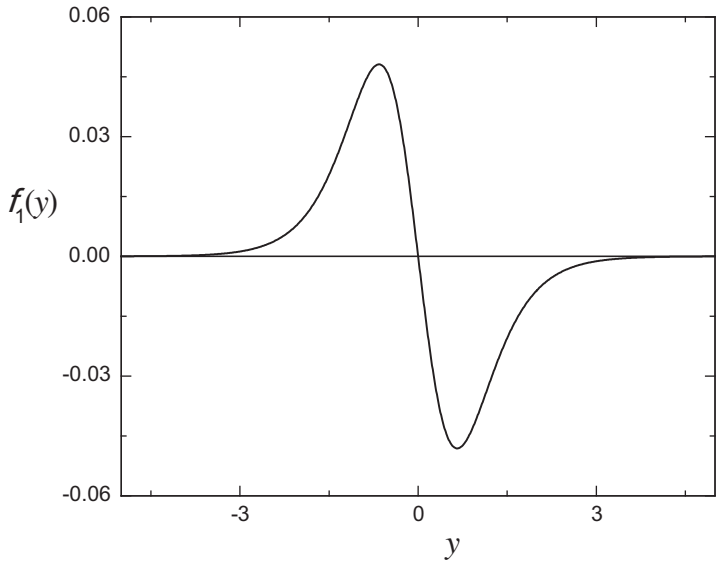

Fig. 5. The function f_1, proportional to the first two terms in Eq. (5), as a function of y.

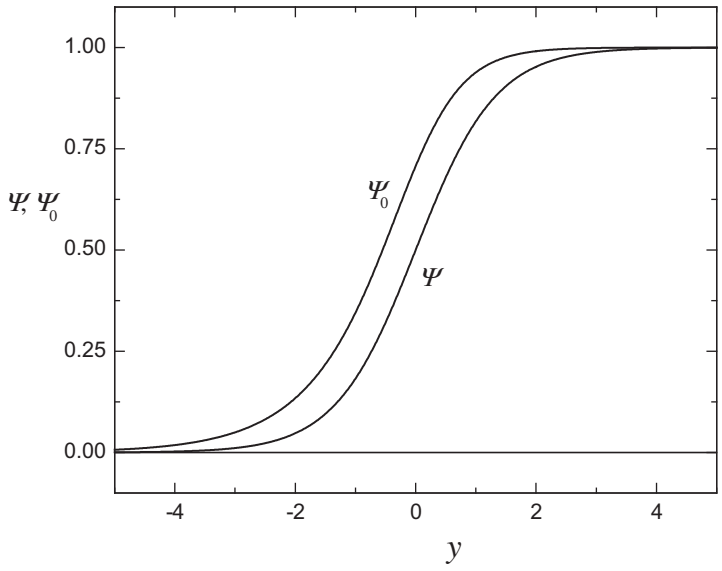

Fig. 6. The functions ψ and ψ_0, corresponding to $\alpha > 0$ and $\alpha = 0$, respectively, as a function of y.

radial direction. Of course, excited dimers will soon spontaneously move back in the initial stable configuration. The pair of these excitations move towards the opposite ends of a single PF initiating the onset of depolymerization on the both sides of the MT.

Importantly, it appears that this localized wave propagates with supersonic velocity, as explained above. A key question is what happens when this wave reaches the positive end of MT. The last dimer has only one neighbour belonging to the same PF. Hence, the big angle of $\sqrt{6}$ radians will not be suppressed in any way and the last dimer will be shifted towards outside. This means that MT starts to crumble and this is what really happens [13,16]. This could be the mechanism for triggering MT instability since its structure is dynamically very unstable. The dimers lifetime in normal cells is in the range of 2–4 h while the complete depolymerisation occurs in a few seconds.

It might be interesting to point out that depolymerisation always starts from the more active biologically positive end, i.e. negatively electrically charged end. This could suggest that the above kinks preferably go towards this MT end.

It is also interesting to consider the possible active role of such conformational kinks in the regulation of intracellular traffic, performed along MTs in terms of two classes of motor proteins, kinesin and dynein. These kinks could facilitate the

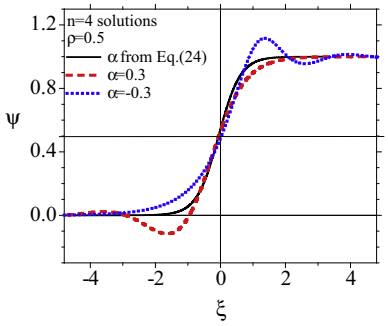

Fig. 7. Numerical solutions of Eq. (8) for the three different values of the parameter α.

attachment of the proper motor for MT providing the onset of transport of different organelles, such as mitochondria, in the cell's compartment where in the need for them.

Acknowledgements

We would like to thank Dejan Milutinović who plotted Fig. 1 and our colleague Dr. Zoran Ivić for inspiring discussions.

This research was supported by funds from Serbian Ministry of Education and Sciences, grants III45010, OI171009 and ON171017.

References

[1] J.A. Tuszyński, S. Hameroff, M.V. Satarić, B. Trpisová, M.L.A. Nip, Ferroelectric behavior in microtubule dipole lattices: implications for information processing, signaling and assembly/disassembly, J. Theor. Biol. 174 (1995) 371–380.
[2] J.A. Tuszyński, J.A. Brown, E. Crawford, E.J. Carpenter, M.L.A. Nip, J.M. Dixon, M.V. Satarić, Molecular dynamics simulations of tubulin structure and calculations of electrostatic properties of microtubules, Math. Comput. Model. 41 (2005) 1055–1070.
[3] M.V. Satarić, R.B. Žakula, J.A. Tuszyński, A model of the energy transfer mechanism in microtubules involving a single soliton, Nanobiology 1 (1992) 445–456.
[4] P. Dustin, Microtubules, Springer, Berlin, 1984.
[5] M.V. Satarić, J.A. Tuszyński, R.B. Žakula, Kinklike excitations as an energy transfer mechanism in microtubules, Phys. Rev. E 48 (1993) 589–597.
[6] M. Cifra, J. Pokorný, D. Havelka, O. Kučera, Electric field generated by axial longitudinal vibration modes of microtubule, BioSystems 100 (2010) 122–131.
[7] D. Havelka, M. Cifra, O. Kučera, J. Pokorný, J. Vrba, High-frequency electric field and radiation characteristics of cellular microtubule network, J. Theor. Biol. 286 (2011) 31–40.
[8] O. Kučera, D. Havelka, Mechano-electrical vibrations of microtubules – link to subcellular morphology, BioSystems 109 (2012) 346–355.
[9] M.V. Satarić, L. Budinski-Petković, I. Lončarević, J.A. Tuszyńsky, Modelling the role of intrinsic electric fields in microtubules as an additional control mechanism of bi-directional intracellular transport, Cell Biochem. Biophys. 52 (2008) 113–124.
[10] D. Havelka, M. Cifra, J. Vrba, What is more important for radiated power from cells-size or geometry?, J Phys.: Conf. Ser. 329 (2011) 012014.
[11] J.E. Schoutens, Dipole-dipole interactions in microtubules, J. Biol. Phys. 31 (2005) 35–55.
[12] S. Zdravković, M.V. Satarić, S. Zeković, Nonlinear dynamics of microtubules – a longitudinal model, Europhys. Lett. 102 (2013) 38002.
[13] L.A. Amos, D. Schlieper, Microtubules and maps, Adv. Protein Chem. 71 (2005) 257–298.
[14] N.R. Watts, N. Cheng, W. West, A.C. Steven, D.L. Sacket, The cryptophycin–tubulin ring structure indicates two points of curvature in the tubulin dimer, Biochemistry 41 (2002) 12662–12669.
[15] F. Pampaloni, E.L. Florin, Microtubule architecture: inspiration for novel carbon nanotube-based biomimetic materials, Trends Biotechnol. 26 (2008) 302–310.
[16] E. Nogales, M. Whittaker, R.A. Milligan, K.H. Downing, High-resolution model of the microtubule, Cell 96 (1999) 79–88.
[17] P. Drabik, S. Gusarov, A. Kovalenko, Microtubule stability studied by three-dimensional molecular theory of solvation, Biophys. J. 92 (2007) 394–403.
[18] M.V. Satarić, L. Matsson, J.A. Tuszyński, Complex movements of motor protein relay helices during the power stroke, Phys. Rev. E 74 (2006) 051902.
[19] S. Zdravković, L. Kavitha, M.V. Satarić, S. Zeković, J. Petrović, Modified extended tanh-function method and nonlinear dynamics of microtubules, Chaos Solitons Fractals 45 (2012) 1378–1386.
[20] A. Gordon, Nonlinear mechanism for proton transfer in hydrogen-bonded solids, Physica B 146 (1987) 373–378.
[21] E. Fan, Extended tanh-function method and its applications to nonlinear equations, Phys. Lett. A 277 (2000) 212–218.
[22] S.A. El-Wakil, M.A. Abdou, New exact traveling wave solutions using modified extended tanh-function method, Chaos Solitons Fractals 31 (2007) 840–852.
[23] A.H.A. Ali, The modified extended tanh-function method for solving coupled MKdV and coupled Hirota–Satsuma coupled KdV equations, Phys. Lett. A 363 (2007) 420–425.
[24] L. Kavitha, N. Akila, A. Prabhua, O. Kuzmanovska-Barandovska, D. Gopi, Exact solitary solutions of an inhomogeneous modified nonlinear Schrödinger equation with competing nonlinearities, Math. Comput. Model. 53 (2011) 1095–1110.
[25] D.L. Sekulić, M.V. Satarić, M.B. Živanov, Symbolic computation of some new nonlinear partial differential equations of nanobiosciences using modified extended tanh-function method, Appl. Math. Comput. 218 (2011) 3499–3506.
[26] N.I. Akhiezer, Elements of the Theory of Elliptic Functions, Translations of Mathematical Monographs, vol. 79, American Mathematical Society, Providence, 1990.
[27] C. Dai, J. Zhang, Jacobian elliptic function method for nonlinear differential-difference equations, Chaos Solitons Fractals 27 (2006) 1042–1047.
[28] S. Zeković, S. Zdravković, L. Kavitha, A. Muniyappan, Employment of Jacobian elliptic functios for solving problems in nonlinear dynamics of microtubules, Chin. Phys. B 23 (2014) 020504.
[29] O. Cornejo-Perez, H.C. Rosu, Nonlinear second order ODE'S: factorizations and particular solutions, Prog. Theor. Phys. 114 (2005) 533–538.

[30] O. Cornejo-Pérez, J. Negro, L.M. Nieto, H.C. Rosu, Traveling-wave solutions for Korteweg-de Vries-Burgers equations through factorizations, Found. Phys. 36 (2006) 1587–1599.
[31] W. Alka, Amit Goyal, C. Nagaraja Kumar, Nonlinear dynamics of DNA–Riccati generalized solitary wave solutions, Phys. Lett. A 375 (2011) 480–483.
[32] S. Zdravković, A. Maluckov, M. Đekić, S. Kuzmanović, M.V. Satarić, Are microtubules discrete or continuum systems? Appl. Math. Comput. (submitted for publication).
[33] N.A. Kudryashov, Exact solitary waves of the fisher equation, Phys. Lett. A 342 (2005) 99–106.
[34] N.A. Kudryashov, Simplest equation method to look for exact solutions of nonlinear differential equations, Chaos Solitons Fractals 24 (2005) 1217–1231.
[35] N.A. Kudryashov, N.B. Loguinova, Extended simplest equation method for nonlinear differential equations, Appl. Math. Comput. 205 (2008) 396–402.
[36] N.A. Kudryashov, N.B. Loguinova, Be careful with the Exp-function method, Commun. Nonlinear Sci. Numer. Simul. 14 (2009) 1881–1890.
[37] N.A. Kudryashov, Seven common errors in finding exact solutions of nonlinear differential equations, Commun. Nonlinear Sci. Numer. Simul. 14 (2009) 3507–3529.
[38] A.S. Davydov, Solitons in Molecular Systems, Mathematics and its Applications, D. Reidel Publishing Company, Dordrecht, 1985.
[39] W.H. Press, S.A. Teukolsky, W.T. Vetterling, B.P. Flannery, Numerical Recipes: The Art of Scientific Computing, 3rd edition., Cambridge University Press, 2007.
[40] S.H. Strogatz, Nonlinear Dynamics and Chaos, Addison-Wesley Publishing Company, Reading, Massachusetts, 1994.